

Molecular Dynamics Study of Silica–Alumina Interfaces

Slawomir Blonski and Stephen H. Garofalini*

Department of Ceramics and Interfacial Molecular Science Laboratory, Institute for Engineered Materials, Rutgers University, P.O. Box 909, Piscataway, New Jersey 08855-0909

Received: June 28, 1995; In Final Form: October 30, 1995[⊗]

Computer simulations of silica–alumina interface formation by a sol-gel process were performed using the molecular dynamics method. The polymerization reaction of silicic acid molecules was simulated for 1 ns (10 000 000 time steps). A complete transformation from liquid silicic acid to dense silica was observed due to removal of water from the sample. The reaction kinetics was characterized using the degree of polymerization of polysiloxane chains and relative concentrations of silicon Q species. Hydroxyl groups originally present on the alumina surface played a crucial role in formation of an ordered atomic structure in the interface region.

Introduction

Alumina is one of the most widely used ceramic materials today.^{1,2} Many of alumina properties are controlled by structure and stability of its surfaces. Moreover, additives interact with the surfaces and modify properties of the alumina materials. We have previously applied molecular dynamics simulations to study the surfaces.³ The simulations have shown how silicon dopants stabilize surfaces of γ -alumina at high temperatures.^{4,5} Silica–alumina solids can also be formed by the sol-gel method.⁶ Such mixed solids are active catalysts and possess acidic character. The acidity is presumed to be generated at the interface between the two components. Several models of the acid sites have been proposed; however, the atomistic structure of the silica–alumina interface was not known before this work.

Silica–alumina interfaces are also present in silica-rich grain boundaries in polycrystalline aluminas. The grain boundary phase originates from sintering aids added during production as well as from impurities present in the raw materials. Although the boundary phase occupies only a small volume percentage of the bulk ceramic, this is an important component of the microstructure that can influence various mechanical and optical properties.^{7–9} The grain boundaries are usually amorphous; however, they can also crystallize after the sintering. Our simulations provide information about atomistic structure of the silica-rich grain boundaries in alumina ceramics. This forms a basis for understanding such phenomena as segregation of calcium and other cations in grain boundary regions.

This paper presents computational molecular dynamics studies of an interface between glassy silica formed by the sol-gel method and hydroxylated, basal (0001) surfaces of the α -alumina crystal. In the following section, the computational procedure is summarized and the potential applied in the model is described. The next section contains a description of the preparation of the initial sample. Kinetics of the polymerization reaction and structures of the formed interfaces are presented in the subsequent sections.

Computational Procedure

Molecular dynamics simulations were performed in the constant-pressure, constant-temperature mode. Pressure was

TABLE 1: Al–O–H Bonding Parameters Obtained from Calculations^a

system	$r_{\text{Al-O}}$ (Å)	$r_{\text{O-H}}$ (Å)	$\angle\text{Al-O-H}$ (deg)
Al(OH) ₃ molecule			
this work	1.65	1.02	168
<i>ab initio</i> ¹⁷	1.68	0.95	163
H ₂ O on α -Al ₂ O ₃ surface			
this work	1.87	1.02	
<i>ab initio</i> ¹⁸	1.89	0.95	
OH+H on α -Al ₂ O ₃ surface			
this work	1.73	1.02	168
<i>ab initio</i> ¹⁸	1.78	0.95	

^a The *ab initio* results of refs 17 and 18 are for the AlOH molecule and the H₂OAlO⁺ cluster, respectively.

controlled using the Berendsen's algorithm,¹⁰ but with the diagonal stress tensor elements decoupled from each other. Temperature control was imposed throughout entire runs for every atom in a system by rescaling velocities after every 20th time step. Newton's equations of motion were integrated using the fifth-order Nordsieck–Gear algorithm. A time step of 0.1 fs was used in the integration. Neighbor lists were used in the calculations of two-body as well as three-body interactions. Simulations were significantly speeded up by applying the link-cell method¹¹ in construction of the neighbor lists. This allowed for a very long simulation of the polymerization reaction with 10 000 000 time steps, although it took about 800 h of CPU time on a Hewlett-Packard workstation Model 9000/750, not including the much shorter time used for the formation and hydroxylation of the alumina crystal surfaces.

Forces applied to atoms were derived from an empirical potential. The interactions in the simulated system were defined by two- and three-body terms of the potential. The total potential energy was obtained by summation of the terms over all possible two- and three-atom combinations. The parameters for the interactions among Al and O atoms were applied from the previous simulations of alumina crystals.^{3,5} The parameters for the interactions among Si, O, and H atoms were applied from the simulations of the polymerization reactions in silica sols.^{12,13} The parameters for the interactions among Al and H atoms were developed in this work on the basis of the parameters for the interactions among Si and H atoms. Following test calculations for the Al(OH)₃ molecule and for a hydroxylation of the (0001) alumina surface (see Table 1), the final Al–H interaction was purely repulsive, but with the strength slightly lowered in comparison to the Si–H pair.

[⊗] Abstract published in *Advance ACS Abstracts*, January 1, 1996.

TABLE 2: Two-Body Parameters

atoms ^a								
<i>i</i>	<i>j</i>	<i>A_{ij}</i> (fJ)	<i>β_{ij}</i> (Å)	<i>ρ_{ij}</i> (Å)	<i>a_{ij}</i> (aJ)	<i>b_{ij}</i> (Å ⁻¹)	<i>c_{ij}</i> (Å)	
O	O	0.072 500	2.34	0.29				
Si	Si	0.187 700	2.30	0.29				
Al	Al	0.050 000	2.35	0.29				
H	H	0.003 400	2.10	0.35	-0.527 93	6.0	1.51	
					+0.034 73	2.0	2.42	
Si	Al	0.252 300	2.33	0.29				
Si	H	0.069 000	2.31	0.29	-4.654 20	6.0	2.20	
Al	H	0.005 000	2.31	0.29				
Si	O	0.296 200	2.34	0.29				
Al	O	0.249 000	2.34	0.29				
H	O	0.039 836	2.26	0.29	-0.208 40	15.0	1.05	
					+0.764 12	3.2	1.50	
					-0.083 36	5.0	2.00	

^a Atom *i* (*q_i*): H (+1); O (-2); Al (+3); Si (+4).

The two-body interactions were generally described by the modified Born–Mayer–Huggins (BMH) potential^{14a} defined by the formula

$$\Phi_{ij}^{\text{BMH}} = A_{ij} \exp(-r_{ij}/\rho_{ij}) + (q_i q_j e^2 / r_{ij}) \operatorname{erfc}(r_{ij}/\beta_{ij})$$

where r_{ij} is the separation distance between ions i and j , e is the elementary charge, and erfc is the complementary error function. The values of the parameters q_i , A_{ij} , β_{ij} , and ρ_{ij} are listed in Table 2. An additional potential was applied for the interactions with H atoms.¹³ That potential consists of up to three terms ($k = 1, 2, 3$) of the following form:

$$\Phi_{ij}^{\text{HX}(k)} = a_{ij}^{(k)} / \{1 + \exp[b_{ij}^{(k)}(r_{ij} - c_{ij}^{(k)})]\}$$

This function, which has the familiar shape of the Fermi–Dirac distribution function, can be called a complementary sigmoidal function. The a_{ij} , b_{ij} , and c_{ij} parameters are also given in Table 2. The cutoff radius of 5.5 Å was applied to the two-body interactions throughout the simulations. Such a short cutoff can be used, because the Coulomb interactions defined by the second term of the BMH potential are tempered by the error function to model the charge-screening effects. Although the potential is short-range, it has allowed for successful simulations of both glassy silica^{12,13,14a–d} and crystalline alumina.^{3–5}

The three-body interactions were defined by the following formula:

$$\Psi_{jik} = \Lambda_{jik} \exp[\gamma_{ij}/(r_{ij} - R_{ij}) + (r_{ik} - R_{ik})] \Omega_{jik}, \quad \text{if } r_{ij} < R_{ij} \text{ and } r_{ik} < R_{ik}$$

$$\Psi_{jik} = 0, \quad \text{if } r_{ij} \geq R_{ij} \text{ or } r_{ik} \geq R_{ik}$$

with $\Lambda_{jik} = \lambda_{ij}^{1/2} \lambda_{ik}^{1/2}$ and the angular part, Ω_{jik} , given by

$$\Omega_{jik} = (\cos \theta_{jik} - \cos \theta_{jik}^0)^2, \quad \text{for Si/Al/H–O–Si/Al/H} \quad \text{and O–Si–O}$$

$$\Omega_{jik} = [(\cos \theta_{jik} - \cos \theta_{jik}^0) \sin \theta_{jik} \cos \theta_{jik}]^2, \quad \text{for O–Al–O}$$

where θ_{jik} is the angle formed by the ions j , i , and k with the ion i placed at the vertex. The parameters for the three-body interactions λ_{ij} , γ_{ij} , R_{ij} , and θ_{jik}^0 are listed in Table 3.

Sample Preparation

All the simulations performed during the initial sample preparation were conducted with the pressure set to the ambient value of 1 atm (0.1 MPa). At the beginning, a bulk crystal of α -alumina consisting of 1800 atoms was simulated at 300 K

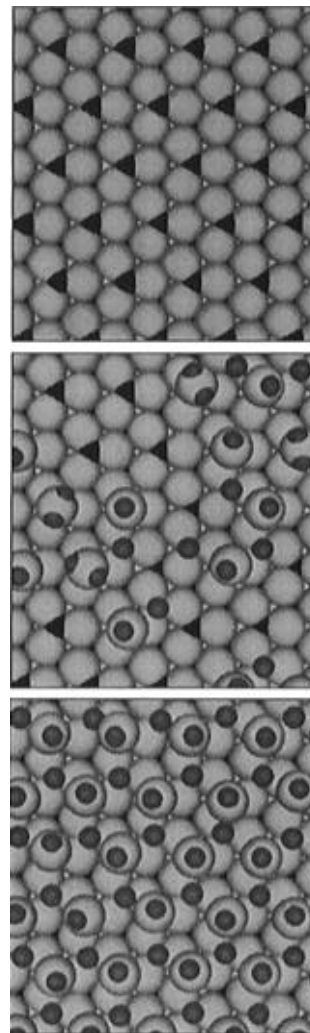


Figure 1. (0001) surface of α -Al₂O₃: (top) a pure surface, (middle) a surface partially covered by water, and (bottom) a completely hydroxylated surface; O, large gray circles; Al, small, black circles (visible as triangles); H, small, gray circles.

TABLE 3: Three-Body Parameters

atoms						
<i>j</i>	<i>i</i>	<i>k</i>	<i>λ_{ij}</i> (fJ)	<i>γ_{ij}</i> (Å)	<i>R_{ij}</i> (Å)	<i>θ_{jik}⁰</i> (deg)
Al/Si	O	Al/Si/H	0.001	2.0	2.6	109.5
O	Al/Si	O	0.024	2.8	3.0	109.5
H	O	Al/Si	0.025	1.2	1.5	109.5
H	O	H	0.035	1.3	1.6	104.5

for 10 ps. After that, the correct, lowest energy, (0001) surfaces³ were exposed on top and bottom of the sample by shifting the atoms within the periodic boundaries. In the next step, periodic boundary conditions in the direction perpendicular to the (0001) surface were abandoned. This step created two basal alumina surfaces with one layer of Al ions outside the layer of O ions (see the top part of Figure 1).³ In the following step, the surfaces were hydroxylated by deposition of water molecules one by one with intervals of 1 ps at 300 K.

The simulation shows that, when a water molecule gets close to the surface, it is adsorbed on one of the Al cations present on the surface and remains intact, that is, an associative adsorption. However, when some energy is delivered to the water molecule, e.g., by collisions with other molecules, a dissociation of H₂O occurs. One of the hydrogens moves away from the OH group and settles above the center of a triangle formed by adjacent oxygens (see the middle part of Figure 1). The dissociated hydrogen diffuses somewhat across the surface before it finds a favored place. A hydroxyl group remains

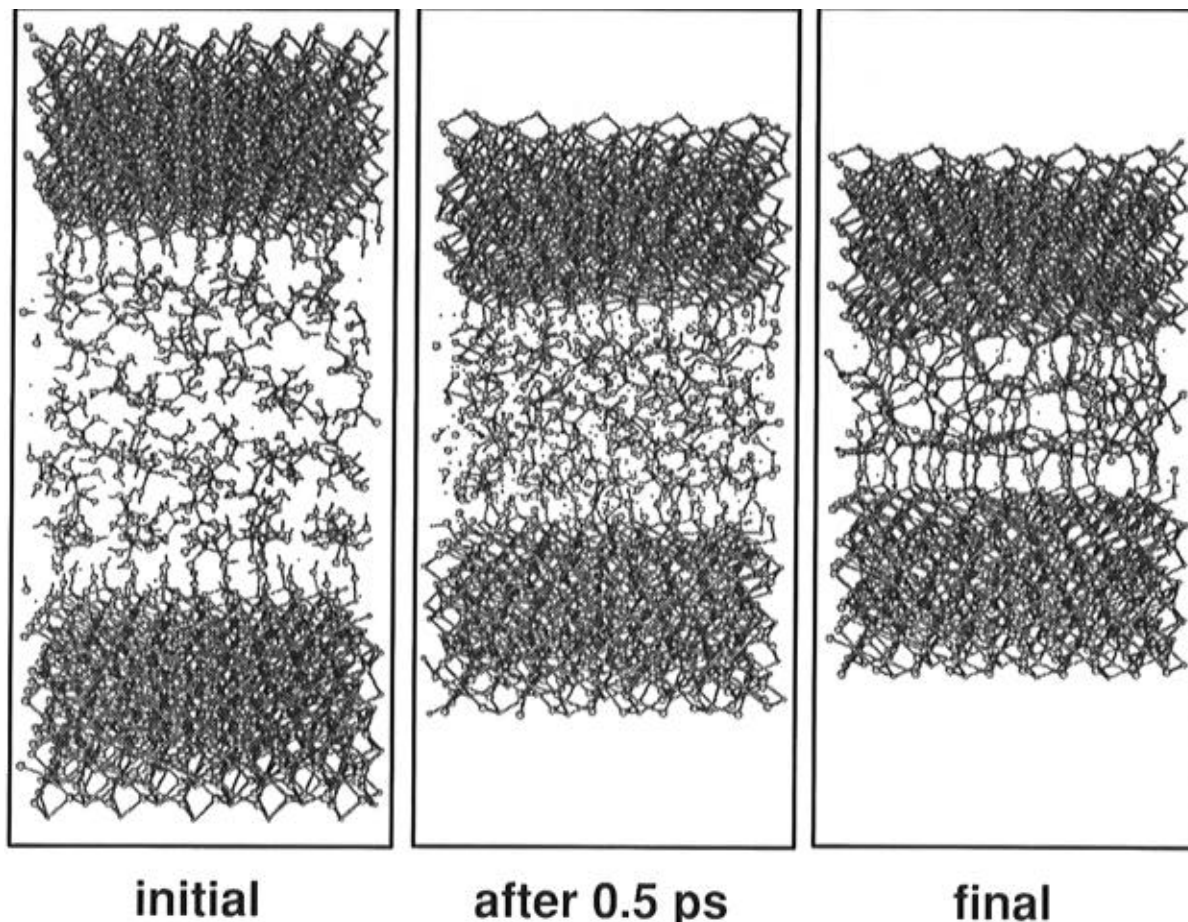


Figure 2. Initial and final configurations of the simulated interface. Alumina crystals are at the top and bottom of the sample.

bonded to the same cation to which the water molecule was attached before the dissociation, but now the adsorption is much stronger. The Al–O bond shortens from 1.87 Å for H₂O on the basal surface of α -Al₂O₃ to 1.73 Å for OH on the same surface (see Table 1).

Adsorbed water should ultimately cover the entire surface. However, such a situation is hard to achieve within the simulated time. When some number of water molecules is adsorbed on the surface and transformed into the OH groups, any new molecule coming to the surface tends to form a hydrogen bond with them rather than stick to the surface. The chainlike structures built in this way make access to the surface even more difficult. So the water layer extends, but the coverage of the surface does not increase. To simulate adsorption more efficiently, the water molecules which were not adsorbed for some period of time were artificially removed from the system. New water molecules were subsequently added. In such a way, completely covered surfaces were obtained. The hydroxylated surface shown in the bottom part of Figure 1 reflects hexagonal symmetry of the pure basal surface of α -alumina. Not only do the OH groups form a lattice induced by the surface Al ions but also the dissociated hydrogen atoms create a regular pattern.

Having done the hydroxylation, the simulation cell was extended in the [0001] direction and 100 silicic acid molecules, H₄SiO₄ (900 atoms), were placed in the empty space between the surfaces. Periodic boundaries were reimposed in the [0001] direction so that the three-dimensional periodic boundary conditions existed. The entire sample was then equilibrated at 300 K for 10 ps, to allow for the relaxation of the liquid silicic acid. The initial configuration of the silicic acid was ordered in a quasi-crystalline manner; however, it quickly became disordered during the relaxation. The equilibration was the final step of the sample preparation, giving two hydroxylated (0001) surfaces of α -alumina separated by H₄SiO₄ molecules.

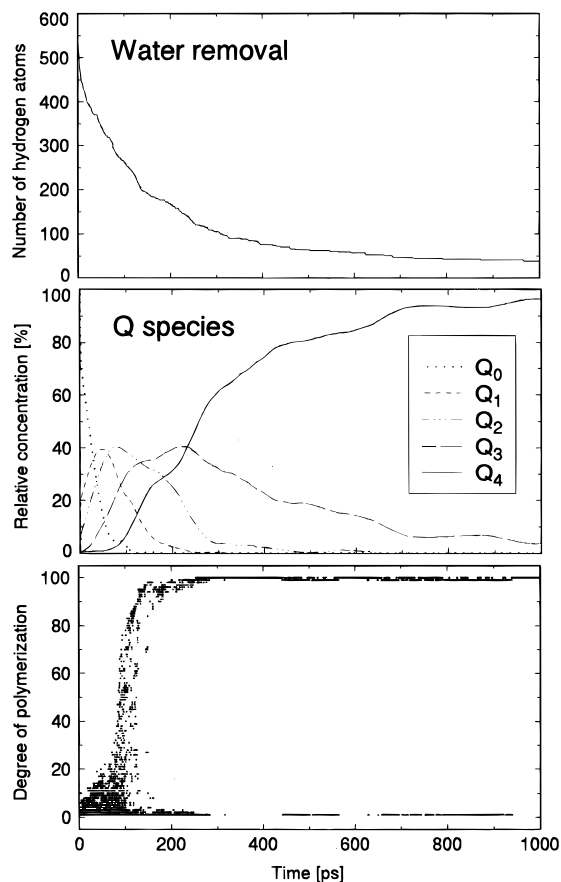


Figure 3. Time dependence of the simulated polymerization reaction measured by water content in the sample (top), relative concentrations of the Q species (middle), and the degree of polymerization of polysiloxane chains (bottom).

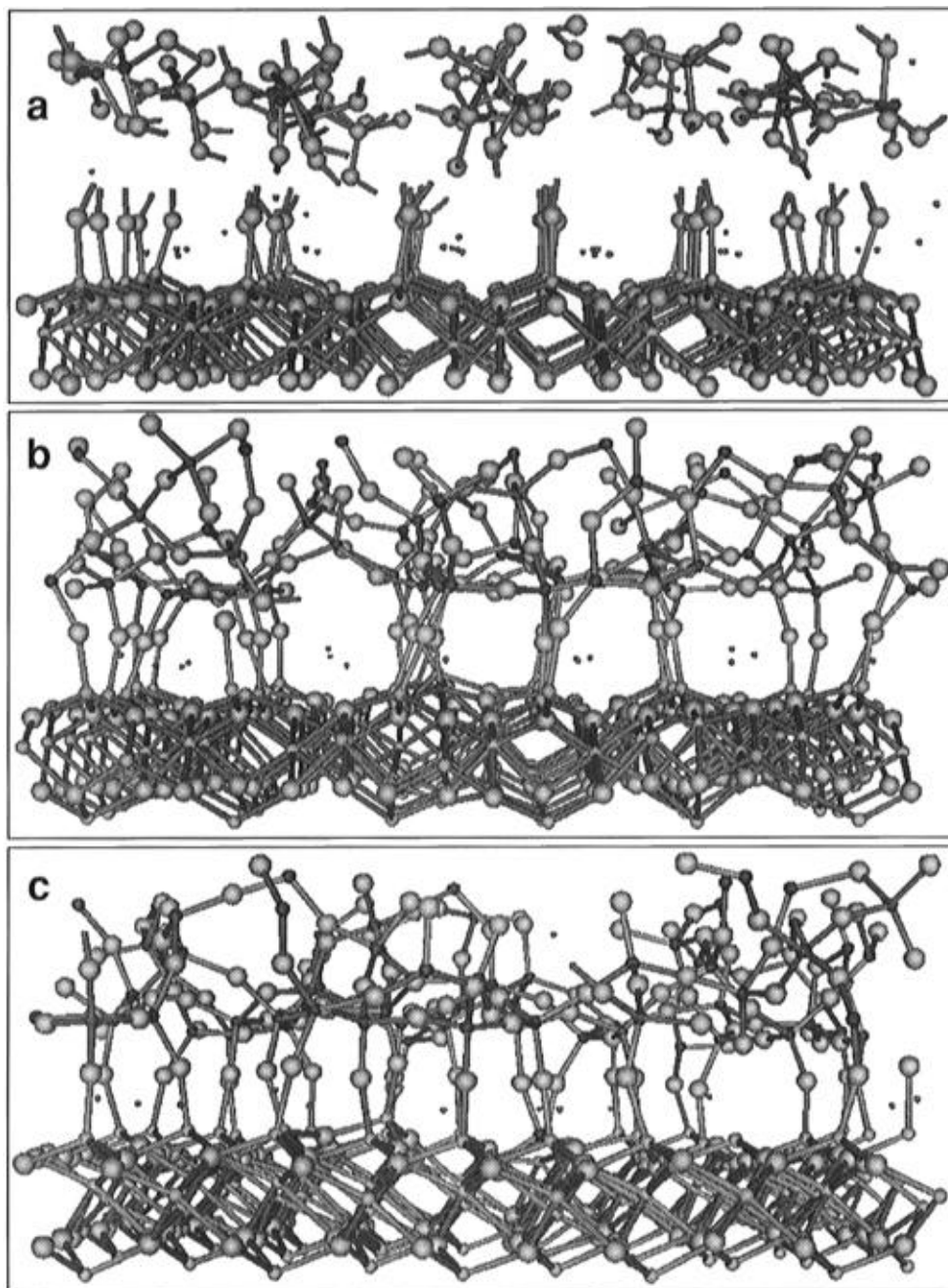


Figure 4. Close-ups of the silica–alumina interface region: (a) the initial configuration, before polymerization; (b) and (c) the final configuration viewed from the mutually perpendicular directions. The largest, gray circles represent oxygen atoms; the smallest, black dots are hydrogen atoms.

Reaction Kinetics

The polymerization simulation was carried out at 2000 K, which allows for observation of the reaction kinetics during a time accessible in molecular dynamics simulations. Although the simulation temperature may seem to be unrealistically high, it is only about 25% of the simulated melting temperature of pure silica with these potentials. During the first 300 ps of the polymerization reaction simulation, a compressing stress of 10^5 atm was imposed on the sample in the direction perpendicular to the surfaces. The pressure prevented uncontrolled expansion of the high-temperature silicic acid. The polymerization reaction was simulated for 1 ns. After that, the sample was relaxed at 300 K for 10 ps. That final run was used for structural analysis of the formed interfaces.

Illustrations of the initial and final configurations of the sample are presented in Figure 2. The left panel shows molecules of silicic acid placed between hydroxylated surfaces of α -alumina surfaces. The disordered character of the liquid

can be clearly observed. The middle panel shows the sample after the quick, initial contraction. The right panel shows the formed silica–alumina interfaces at the end of the simulation. Dense silica gel binds the alumina surfaces together. Figure 2 also displays that the sample shrunk during the polymerization. This happened mainly during the initial 300 ps of the simulation, when the stress was imposed on the sample. It was accompanied by removal of water from the sample. After every 1 ps of the simulation, the sample was checked for the presence of water molecules and unbonded hydroxyl groups. When an H_2O molecule was found, it was removed from the sample. When an OH group was found, it was also removed from the sample together with a closest, unbonded hydrogen atom. In such a way, only stoichiometric water was removed and the charge balance in the sample was preserved. The top part of Figure 3 shows the history of water removal measured by the number of hydrogen atoms remaining in the sample. Most of the water (about 200 molecules) was removed during the initial

300 ps of the polymerization. During the next 700 ps only about 30 additional H₂O molecules were removed. At the final stage, there remained in the sample an equivalent of 19 water molecules, all in the form of bonded OH groups and unbonded H atoms.

Water appeared in the sample as a result of a polymerization reaction similar to



This reaction can be also characterized in terms of Q species: two Q₀'s are transformed into two Q₁'s with creation of a water molecule (Q species are the species of silicon ions; the subscript *n* in Q_{*n*} indicates the number of bridging oxygen ions bonded to a silicon ion; here an oxygen ion is considered bridging when it binds a Si ion with another Si or Al ion). Reactions with higher order Q species also occur and result in the creation of water molecules. Concentration of different Q species is an important indicator of the polymerization reaction kinetics because it can be measured by experimental techniques such as NMR.¹³ The middle part of Figure 3 shows relative concentrations of Q species calculated from the simulation. Initially, only Q₀'s were in the sample. They disappeared quickly during the first 100 ps of the polymerization reaction. Then Q₁'s and Q₂'s were mainly formed, but they were also replaced soon by Q₃'s and Q₄'s. After about 250 ps, only the number of Q₄'s was increasing: All the other Q species were vanishing. At the end of the simulation, 96% of Si ions were of the Q₄ kind, and only 4% were Q₃. Full conversion to Q₄'s is expected in the longer time, which is however beyond the limits of the current simulation.

Kinetics of the polymerization reaction can also be characterized by the degree of polymerization of the polysiloxane chains occurring in the sample. The chains under consideration, oligomers rather than polymers, do not need to be linear. The structure of the silicic acid molecule allows for frequent branching. The degree of polymerization is measured by counting the number of Si ions in a chain. In the sample containing 100 Si ions there may be many chains with various degrees of polymerization (initially, there were 100 chains of degree 1). Time evolution of the degree of polymerization is shown on the graph in the bottom part of Figure 3. On the graph, points were drawn only at those coordinates for which there was at least one chain with a given degree of polymerization at a given time. The graph shows that during the initial 80–90 ps of the polymerization only short chains were formed. This changed dramatically around 100 ps: The short chains combined to form longer ones. After that, one long chain dominated the sample and reacted with very short chains with a slower pace. After about 300 ps, only one chain remained in the sample: All the Si ions were in a silica network.

Interface Structure

Figure 4b shows a close-up illustration of the silica–alumina interface obtained in the simulation. Between the alumina surface and the silica glass, there is an ordered layer of bridging oxygen ions which bind the two different materials. The anions

were originally in the hydroxyl groups bonded to the surface (see Figure 4a). Not only was the ordered configuration of the surface OH groups preserved but it also influenced the silica in contact with the alumina. Many Si–O bonds in this region are oriented parallel to the alumina surface. The bonds form cage-like structures in the interface region. This can be seen both from the point of view used in Figure 4b and from the perpendicular direction in Figure 4c. The cages attracted hydrogen ions. Most of the H ions which remained after the water removal occupy the cages. They can be seen in Figure 4 as the very small circles.

Conclusions

Molecular dynamics simulations show that, in the initial stages of the silicic acid polymerization reaction, only short chains (oligomers) are formed. At some point, the short chains combine rather abruptly to create long, branched chains which are finally transformed into a three-dimensional network. This resembles a percolation phenomenon expected in the gelatin process.^{15,16} In the final structure, the silica gel is chemically bonded to the alumina surfaces. An interface between glassy silica and crystalline alumina has an ordered region. In the ordered region, atoms and bonds between them form cage-like structures which provide excess volume for hydrogen atoms and other cations. The light cations diffuse into the cages and concentrate at the interface. This model describes not only interfaces in silica–alumina mixed solid–acids but also silica-rich grain boundaries in polycrystalline alumina materials.

Acknowledgment. The authors gratefully acknowledge support from the Center for Ceramic Research at Rutgers University.

References and Notes

- (1) Gitzen, W. H. *Alumina as a Ceramic Material*; American Ceramic Society: Columbus, OH, 1970.
- (2) Dörre, E.; Hübner, H. *Alumina: Processing, Properties, and Applications*; Springer: Berlin, 1984.
- (3) Blonski, S.; Garofalini, S. H. *Surf. Sci.* **1993**, *295*, 263.
- (4) Blonski, S.; Garofalini, S. H. *Chem. Phys. Lett.* **1993**, *211*, 575.
- (5) Blonski, S.; Garofalini, S. H. *Catal. Lett.* **1994**, *25*, 325.
- (6) Katada, N.; Toyama, T.; Niwa, M. *J. Phys. Chem.* **1994**, *98*, 7647.
- (7) Baik, S.; Moon, J. H. *J. Am. Ceram. Soc.* **1991**, *74*, 819.
- (8) Powell-Dogan, C. A.; Heuer, A. H. *J. Am. Ceram. Soc.* **1994**, *77*, 2593.
- (9) O'Donnell, H. L.; Readey, M. J.; Kovar, D. *J. Am. Ceram. Soc.* **1995**, *78*, 849.
- (10) Berendsen, H. J. C.; Postma, J. P. M.; van Gunsteren, W. F.; DiNola, A.; Haak, J. R. *J. Chem. Phys.* **1984**, *81*, 3684.
- (11) Allen, M. P.; Tildesley, D. J. *Computer Simulation of Liquids*; Clarendon: Oxford, 1990.
- (12) Feuston, B. P.; Garofalini, S. H. *J. Phys. Chem.* **1990**, *94*, 5351.
- (13) Garofalini, S. H.; Martin, G. *J. Phys. Chem.* **1994**, *98*, 1311.
- (14) (a) Feuston, B. P.; Garofalini, S. H. *J. Chem. Phys.* **1988**, *89*, 5818. (b) Melman, H.; Garofalini, S. H. *J. Non-Cryst. Solids* **1991**, *134*, 107. (c) Feuston, B. P.; Garofalini, S. H. *J. Appl. Phys.* **1990**, *68*, 4830. (d) Zirl, D. M.; Garofalini, S. H. *J. Am. Ceram. Soc.* **1990**, *73*, 2848.
- (15) Flory, P. J. *J. Am. Chem. Soc.* **1941**, *63*, 3083.
- (16) Grimmer, G. *Percolation*; Springer-Verlag: New York, 1989.
- (17) Hirota, F.; Tanimoto, M.; Tokiwa, H. *Chem. Phys. Lett.* **1993**, *208*, 115.
- (18) Mejias, J. A.; Oviedo, J.; Fernandez Sanz, J. *Chem. Phys.* **1995**, *191*, 133.